50. Resonances

Revised August 2021 by D.M. Asner (BNL) and C. Hanhart (Jülich).

50.1 General Considerations

Perturbative methods can be applied to systems of quarks and gluons only for large momentum transfers (see review on 'Quantum Chromodynamics') and, under certain conditions, to some properties of systems that contain heavy quarks or very large momentum scales (see review on "Heavy-quark and soft-collinear effective theory"). Dealing with Quantum Chromodynamics (QCD) in the low momentum transfer region is a very complicated, non-perturbative problem. Accordingly, most hadrons are resonances, which means that they appear as poles of the S-matrix in the complex plane on unphysical sheets. These resonances can show up either in so-called formation experiments,

$$A + B \to \mathbf{R} \to C_1 + ... + C_n \ ,$$

where they become visible in an energy scan (for example, the R-function measured in e^+e^- annihilations — *cf.* the corresponding plots in the review on "Plots of Cross Sections and Related Quantities"), or together with a spectator particle S in production experiments of the kind

$$\begin{aligned} A + B \to \mathbf{R} + S \to [C_1 + ... + C_n] + S \ , \\ Z \to \mathbf{R} + S \to [C_1 + ... + C_n] + S \ , \end{aligned}$$

where the first reaction corresponds to an associated production, the second is a decay (see "Review of Multibody Charm Analyses"). In the latter case, the resonance properties are commonly extracted from a Dalitz-plot analysis (see review on "Kinematics") or projections thereof.

Resonance phenomena are very rich: while typical hadronic widths are of the order of 100 MeV (*e.g.*, for the meson resonances $\rho(770)$ or $\psi(4040)$ or the baryon resonance $\Delta(1232)$) corresponding to a lifetime of 10^{-23} s, the widths can also be as small as a few MeV (*e.g.* of $\phi(1020)$ or J/ψ) or as large as several hundred MeV (*e.g.* of the meson resonances $f_0(500)$ or $D_1(2430)$ or the baryon resonance $N(2190)$).

Typically, a resonance appears as a peak in the total cross section. If the structure is narrow and if there are no relevant thresholds or other resonances nearby, the resonance properties may be extracted employing a Breit–Wigner parameterization, if necessary improved by using an energy-dependent width (*cf.* Sec. 50.3.1 of this review). However, in general, unitarity and analyticity call for the use of more refined tools. When there are overlapping resonances with the same quantum numbers, the resonance terms should not simply be added but combined in a non-trivial way either in a K-matrix approach (*cf.* Sec. 50.3.2 of this review) or using other advanced methods (*cf.* Sec. 50.3.6 of this review). Additional constraints from the S-matrix allow one to build more reliable amplitudes and, in turn, to reduce the systematic uncertainties of the resonance parameters: pole locations and residues. In addition, for broad resonances there is no direct relation between pole location and the total width/lifetime — then, the pole residues need to be used in order to quantify the decay properties.

For simplicity, throughout this review the formulas are given for resonances in a system of distinguishable, scalar particles. The additional complications that appear in the presence of spins can be controlled in the helicity framework developed by Jacob and Wick [1], or in a non-covariant [2] or covariant [3] tensor-operator formalisms. Within these approaches, sequential (cascade) decays are commonly treated as a coherent sum of two-body interactions. Most of the expressions below are given for two-body kinematics.

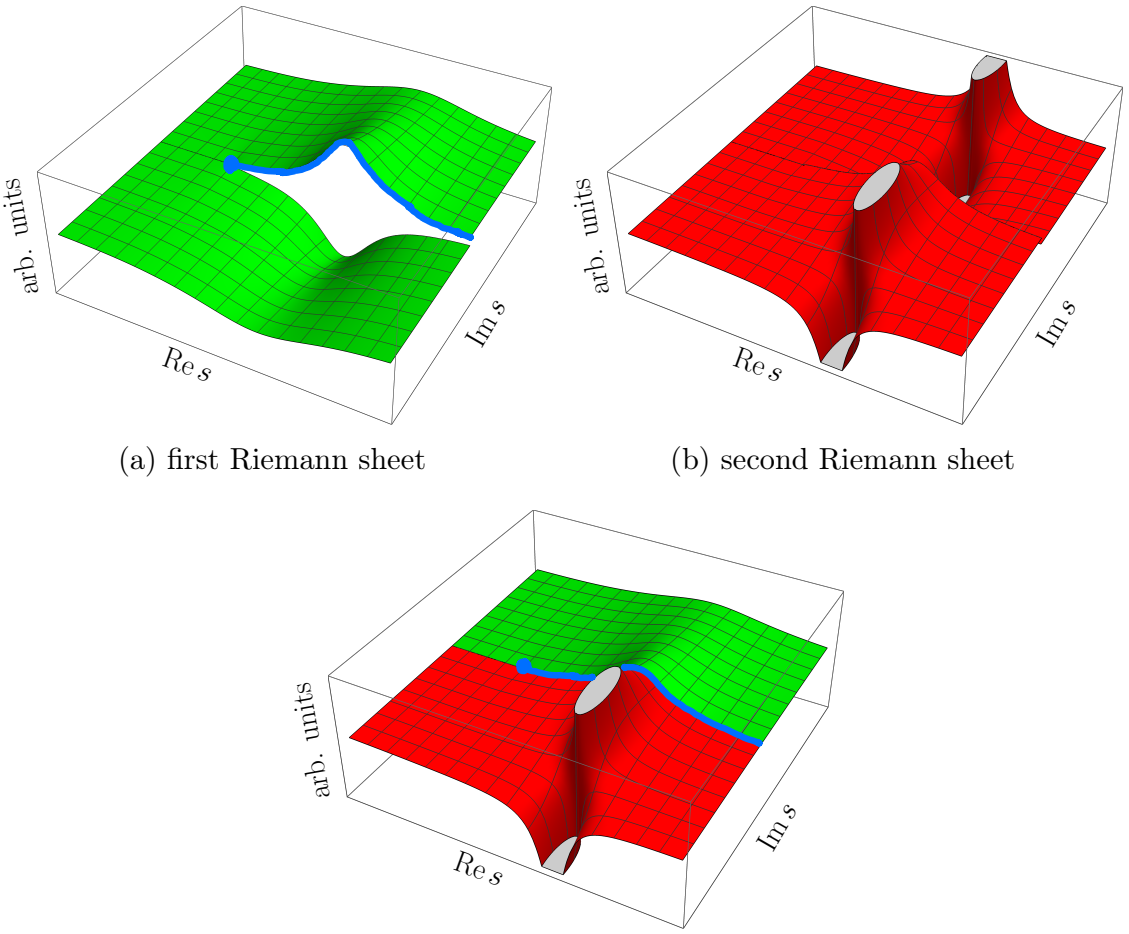

(a) first Riemann sheet

(b) second Riemann sheet

(c) transition from first to second Riemann sheet

Figure 50.1: Imaginary part of a typical single-channel scattering amplitude with an isolated resonance. The blue line shows the physical range of the Mandelstam variable s: it is real and starts from the threshold shown by the blue dot. Plot (a) shows the imaginary part of the amplitude in the complex s-plane that corresponds to the first or physical sheet (green surface), plot (b) shows the related unphysical or the second sheet (red surface) which contains the resonance poles, and plot (c) shows the analytic continuation of the same amplitude from the upper half plane of the physical sheet to the lower half plane of the unphysical sheet. The two sheets are connected smoothly along the real axis above the threshold.

50.1.1 *Properties of the S-matrix*

The unitary operator that connects asymptotic *in* and *out* states is called the S-matrix. The scattering amplitude is defined as the interacting part of the S matrix. For a two-particles scattering process, it reads:

$$i(2\pi)^4\delta^4(p_1+p_2-p_1'-p_2')\,\mathcal{M}(p_1,p_2;p_1',p_2')_{ba} = {}_{\text{out}}\langle p_1'p_2',b|\,S-1\,|p_1p_2,a\rangle_{\text{in}} \tag{50.1}$$

where $|p_1p_2,a\rangle$ and $|p_1'p_2',b\rangle$ are asymptotic states of two non-interacting particles with momentum p_1, p_2 and p_1', p_2'. The channel labels a and b are multi-indices specifying all additional properties

of the channel. In general, $\mathcal{M}$ is a matrix in channel space. For a single-particle state, we employ the relativistic normalization,

$$\langle p'|p\rangle = (2\pi)^3 2E_p\,\delta^3(\vec{p}\,' - \vec{p}), \tag{50.2}$$

with $E_p = \sqrt{\vec{p}^{\,2} + m^2}$. The Mandelstam variables $s = (p_1 + p_2)^2$, $t = (p_1 - p_1')^2$, and $u = (p_1 - p_2')^2$ are the invariant variables describing the scattering. With these definitions the process in Eq. (50.1) is referred to as the s-channel scattering, where the total energy of the interacting system is given by $\sqrt{s}$, while the variable t is related to the scattering angle, *i.e.* the angle between the momenta of the particles 1 and $1'$ in the center-of-momentum frame. The variable u is not independent of s and t, but the relation

$$s + t + u = m_1^2 + m_2^2 + m_{1'}^2 + m_{2'}^2$$

holds, where the m_i denote the masses of the incoming and outgoing particles, $i \in 1, 1', 2, 2'$. Therefore, the reaction amplitude is a function of two variables, $\mathcal{M}(s,t)$. The function $\mathcal{M}(s,t)$ is a multi-valued function due to the complex branch points in the Mandelstam variables. Branch points appear whenever there is a channel opening. Each two-particle threshold introduces a square-root singularity and the number of Riemann sheets doubles. For resonances coupled to multi-particle states with odd number of particles the threshold branch point is logarithmic [4]. The branch points appear in the complex plane of an unphysical sheet when there is a resonance in a subsystem of the final-state particles [4]. The cuts related to the openings of the crossed channels are located on the left-hand side of the complex plane, and, therefore, are referred to as the left-hand cuts. Triangle topologies can induce logarithmic branch points on the unphysical sheets often called triangle singularities (TS) [4–6].

Poles of reaction amplitude refer either to bound states or to resonances. The former poles are located on the physical sheet, the latter are located on unphysical sheets. Naturally, those located on the unphysical sheet closest to the physical one, often called the second sheet, have usually the largest impact on observables. Moreover, as follows from analyticity, if there is a pole at some complex value of s, there must be another pole at its complex conjugate value, s^*. For a single-channel case this is illustrated in Fig. 50.1: the pole with a negative imaginary part is closer to the physical axis and thus influences the observables in the vicinity of the resonance region more strongly. However, at the threshold both poles are equally distant and accordingly equally important. Any of these singularities can lead to some structure in the observables (see also Ref. [7]). If certain kinematical constraints are met, especially the TS can mimic resonance signals, as claimed in Refs. [8–13] or cause significant changes of resonance signals [14]. In addition to not all bumps being resonances, not every resonance generates a bump in all observables. For instance, there is no clear trace of the $N(1440)1/2^+$, the so called Roper resonance, in the πN observables or phase shifts, although careful analyses reveal a pole [15].

In case of two relevant channels we are faced with four Riemann sheets. Then, the sheet that is the closest to the physical axis changes, as the energy increases. This can be seen from the illustration in Fig. 50.2: for energies higher than the first, but lower than the second threshold, the sheet that connects smoothly to the upper half plane of the physical sheet (11) is sheet (21). However, for energies above the second threshold this role is taken over by sheet (22). Accordingly, a pole on sheet (21), but above the second threshold, will show up in data only as a cusp exactly at the second threshold. Sheet (12), on the other hand, is remote for all energies.

The analyticity principle of the S-matrix forbids any singularities on the first Riemann sheet except poles and branch points on the real axis. Unitarity constrains the imaginary part of the amplitude on the real axis as further discussed in the following section. Further constraints come, *e.g.*, from crossing symmetry and duality [16]. Approaches based on analyticity and crossing symmetry, implemented via dispersion theory, like the Roy equations [17] or variants thereof, were

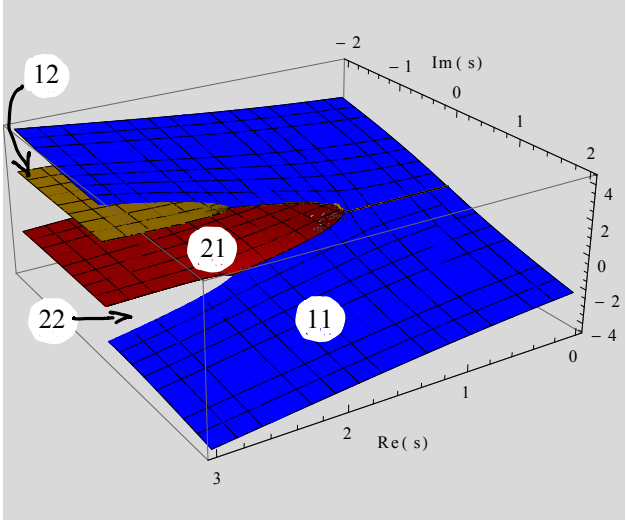

Figure 50.2: Cut structure of the S-matrix in the presence of two-channels. The four sheets are labelled as (ij) with $i = 1, 2$ and $j = 1, 2$ referring to the doubling of the sheets at the first and the second thresholds, respectively.

developed and applied to $\pi\pi \to \pi\pi$ scattering [18–20], πK scattering [21], $\gamma\gamma \to \pi\pi$ [22] as well as pion-nucleon scattering [23, 24].

50.1.2 *Consequences from unitarity*

In what follows, scattering amplitudes, $\mathcal{M}$, and production amplitudes, $\mathcal{A}$, will be distinguished, since unitarity puts different constraints on these. For the scattering amplitude, all considered channels are supposed to be of comparable importance, while for the production amplitudes we require that the initial state is only weakly coupled and, therefore, the probability of the time-reversed reaction is negligibly small compared to the other coupled channels. Most of the strong-interaction processes are then described by the scattering amplitude, *e.g.* $\pi^+\pi^- \to K\bar{K}$, or $D^0\bar{D}^0 \to D^0\bar{D}^0$. Examples for production processes are $e^+e^- \to \pi^+\pi^-$, $\tau \to K^-\pi^0\nu$, $B^0 \to J/\psi\pi^+\pi^-$.

Unitarity of the S matrix, $S^\dagger S = 1$, which is equivalent to the conservation of probability, translates to a constraint for the imaginary part of the reaction amplitude. The amplitude is real below the first threshold. Above the threshold, the discontinuity across the cut related to the threshold branch point, obeys the relation [25]:

$$\mathcal{M}_{ba} - \mathcal{M}^*_{ab} = i\,(2\pi)^4 \sum_c \int d\Phi_c \mathcal{M}^*_{cb}\mathcal{M}_{ca}\ , \tag{50.3}$$

where Φ_c is the invariant phase space for channel c. The sum includes only open channels, *i.e.* those for which the production threshold is below the energy of the scattered system. Complementary, the channels with the threshold higher than the energy of the system are called closed. Using time-reversal symmetry, and $\mathrm{Disc}\,\mathcal{M}(s,t) = 2i\,\mathrm{Im}(\mathcal{M}(s + i\epsilon, t))$ for the s-channel, the optical theorem follows:

$$\mathrm{Im}\,\mathcal{M}_{aa}(s,0) = 2q_a\sqrt{s}\,\sigma_{\mathrm{tot}}(a \to \text{anything})\,. \tag{50.4}$$

Here, q_a is the momentum of particles in their center-of-momentum frame,

$$q_a = \frac{\lambda^{1/2}(s, m^2_{1,a}, m^2_{2,a})}{2\sqrt{s}}\ , \tag{50.5}$$

where $\lambda(x,y,z) = x^2 + y^2 + z^2 - 2xy - 2yz - 2yx$ is the Källén function, $m_{1,a}$ and $m_{2,b}$ are the masses of the two particles in the channel a, *cf.* Eq. (17) of the review on "Kinematics". The value $t = 0$ in Eq. (50.4) corresponds to forward scattering.

The unitarity relation for a production amplitude for a channel a is given by

$$\mathcal{A}_a - \mathcal{A}_a^* = i\,(2\pi)^4 \sum_c \int d\Phi_c \mathcal{M}_{ca}^* \mathcal{A}_c\,. \tag{50.6}$$

Note that production amplitude written as a linear combination of the scattering amplitudes satisfies Eq. (50.6) due to Eq. (50.3). This solution are often practical, especially, when the scattering matrix is well known, as for example for $\pi\pi$ system below 1.1 GeV [26, 27]. However, it should be understood that this kind of treatment is only approximate, since it imports the analytic structure of the scattering amplitude including its left-hand cuts to the production amplitude which in general has a different cut structure. A more sophisticated application of the two-body-unitarity constraints from Eq. (50.6) is the Khuri-Treiman framework often employed to study three-body decays [28]. The standard procedure here is to derive the equations for the production amplitude for small values of the mass of the decaying particle in the scattering domain and relate it to the decay kinematics by an analytic continuation in the decay mass. The method was successfully applied to various decays of light mesons, $\eta \to 3\pi$ in Refs. [29–34], $\phi/\omega \to 3\pi$ in Ref. [35, 36], $\eta' \to \eta\pi\pi$ in Ref. [37], as well as to the charm-mesons decays $D^+ \to K^{0/-}\pi^{0/+}\pi^+$ [38, 39].

50.1.3 *Partial-wave decomposition*

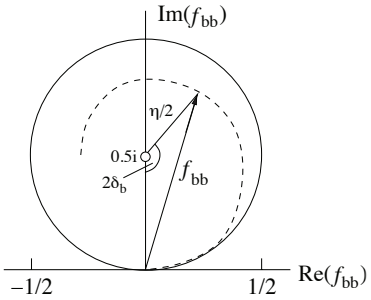

Figure 50.3: Argand plot showing a diagonal element of a partial-wave amplitude, a_{bb}, as a function of energy. The amplitude leaves the unitary circle (solid line) as soon as inelasticity sets in, $\eta < 1$ (dashed line).

It is often convenient to expand the scattering amplitude in partial waves. Since resonances have a well-defined spin, they appear only in a specific partial wave of the reaction amplitude. For scalar particles the expansion reads:

$$\mathcal{M}_{ba}(s,t) = \sum_{j=0}^{\infty} (2j+1)\mathcal{M}_{ba}^j(s) P_j(\cos(\theta))\ , \tag{50.7}$$

where j denotes the total angular momentum and the $P_j(\cos(\theta))$ denotes the Legendre polynomials. In the presence of spins an expansion more complicated than Eq. (50.7) is necessary. In the absence of spins the parameter j coincides with the orbital angular momentum of the particle pairs in the initial and the final state. To simplify notations we will drop the label j for the single-argument function $\mathcal{M}_{ba}(s)$. The unitarity constraint for $\mathcal{M}_{ba}(s)$ reads,

$$\mathrm{Im}\,\mathcal{M}_{ba}(s) = \sum_c \mathcal{M}_{cb}(s)^*\,\rho_c(s)\,\mathcal{M}_{ca}(s) \tag{50.8}$$

with $\rho_c(s)$ being a factor that is related to the two-body phase space in Eq. (12) of the review on "Kinematics",

$$\rho_c(s) = \frac{(2\pi)^4}{2} \int \mathrm{d}\Phi_2 = \frac{1}{16\pi} \frac{2|\vec{q}_c|}{\sqrt{s}} \ , \tag{50.9}$$

with the momentum q_c being defined in Eq. (50.5). Note that in case of the two particles being identical the inclusion of symmetry factors becomes necessary. The partial-wave amplitude $f_{ba}(s)$ is introduced via

$$f_{ba}(s) = \sqrt{\rho_b}\, \mathcal{M}_{ba}(s)\, \sqrt{\rho_a} \ . \tag{50.10}$$

From the unitarity condition Eq. (50.8) it follows that $\mathrm{Im}\, f_{ba}^{-1} = -\delta_{ba}$. Moreover, $\mathbb{I} + 2if$ is a unitary matrix. Hence, the diagonal elements of f can be parameterized as,

$$f_{bb} = (\eta_b \exp(2i\delta_b) - 1)/2i \ , \tag{50.11}$$

where δ_b denotes the phase shift for the scattering from channel b to channel b, η_b is elasticity parameter — also called inelasticity. One has $0 \leq \eta_b \leq 1$, where $\eta_b = 1$ is referred to as a purely elastic scattering. The evolution of the partial-wave amplitude f_{bb} with energy can be displayed as a trajectory in the Argand plot, as shown in Fig. 50.3. In case of a two-channel problem, $\eta_b = \eta_a = \eta$, and the off-diagonal element is $f_{ba} = \sqrt{1-\eta^2}/2\, \exp(i(\delta_b + \delta_a))$. The unitarity condition Eq. (50.11) sets the limit to the squared amplitude f_{bb}:

$$|f_{bb}|^2 = \frac{1}{4}(\eta_b^2 - 2\eta_b \cos(2\delta_b) + 1) \leq \frac{1}{4}(\eta_b + 1)^2 \ , \tag{50.12}$$

where the maximum value is achieved for $\delta_b = \pi/2$. For the partial-wave-projected scattering amplitude the unitarity bound reads:

$$|\mathcal{M}_{bb}| \ \leq \ \frac{1}{2\rho_b}(\eta_b + 1) \ \leq \ \frac{8\pi}{q_b}\sqrt{s}\,, \tag{50.13}$$

where the second inequality comes from $\eta_b \leq 1$. For energies much larger than the masses of the scattering particles. One finds that the upper bound for $|\mathcal{M}_{bb}|$ tends to 16π for large s.

The partial-wave-projected production amplitude $\mathcal{A}(s)$ (the label j is dropped for consistency) is also constrained by unitarity. From Eq. (50.6) it follows:

$$\mathrm{Im}\, \mathcal{A}_a = \sum_b \mathcal{M}_{ba}^*\, \rho_b\, \mathcal{A}_b \ , \tag{50.14}$$

where the sum runs over all open channels. For elastic processes, the sum collapses to the channel a. In this case, the phase of $\mathcal{A}_a$ must agree with the phase of $\mathcal{M}_{aa}$ since the left-hand side of Eq. (50.14) is a real number. The statement is known as the Watson theorem [40].

50.2 Properties of resonances

The main characteristics of a resonance is its pole position in the complex s-plane, s_R. The pole mass M_R and pole width Γ_R are introduced via the pole parameters

$$\sqrt{s_\mathrm{R}} = M_\mathrm{R} - i\Gamma_\mathrm{R}/2 \ . \tag{50.15}$$

Note that the standard Breit–Wigner parameters M_BW and Γ_BW, also introduced below, in general, deviate from the pole parameters, *e.g.*, due to finite width effects and the influence of thresholds. It should be stressed, however, that the pole location s_R as well as the pole residues to be introduced below, are the only resonance properties that are model- and parametrisation independent.

In addition to the pole position, a resonance is characterized by its couplings to the various channels called residues. The Baryon Particle Listings give the elastic pole residues and normalized transition residues. However, different conventions are used in the two sectors, which are shortly outlined here.

In the close vicinity of the resonance pole the scattering matrix $\mathcal{M}$ can be written as

$$\lim_{s\to s_R}(s-s_R)\mathcal{M}_{ba} = -\mathcal{R}_{ba}\ . \tag{50.16}$$

The residues are calculated via an integration along a closed contour around the pole using

$$\mathcal{R}_{ba} = -\frac{1}{2\pi i}\oint ds\mathcal{M}_{ba}\ . \tag{50.17}$$

The factorization of the residue $(\mathcal{R}_{ba})^2 = \mathcal{R}_{aa}\times\mathcal{R}_{bb}$ allows one to introduce pole couplings according to

$$\tilde{g}_a = \mathcal{R}_{ba}/\sqrt{\mathcal{R}_{bb}}\ . \tag{50.18}$$

The pole couplings characterize the transition strength of a given resonance to some channel a independently of how the particular resonance was produced. For a two-particle decays in the S-wave, one may define a partial width and a branching fraction for a resonance via

$$\Gamma_{\mathrm{R}\to a} = \frac{|\tilde{g}_a|^2}{M_{\mathrm{R}}}\rho_a(M_{\mathrm{R}}^2) \quad \text{and} \quad \mathrm{Br}_a = \Gamma_{\mathrm{R}\to a}/\Gamma_{\mathrm{R}}\ , \tag{50.19}$$

where M_{R} and Γ_{R} were introduced in Eq. (50.15). This expression was used to define a two-photon width for the broad $f_0(500)$ [41, 42] as well as in the corresponding section of the Meson Particle Listings. Analogously, one should use residues to quantify the coupling of resonances to certain production channels [43]. For an application of this formalism to the coupling of the $K_0^*(1430)$ resonance to a leptonic current see Ref. [44]. Equation (50.19) defines a partial-decay width independent of the reaction used to extract the parameters. For a narrow resonances it maps smoothly onto the other common definition of the branching fraction, discussed in Eq. (50.20) more closely related to observables. For broad, overlapping resonances, however, it should be understood that Eq. (50.19) serves the purpose to convert the residues to quantities that allow for a more direct comparison of resonance transitions to different channels. In case of resonances with significant couplings to channels that are still closed at the resonance mass, Eq. (50.19) cannot be used since the phase-space factor yields zero.

In the baryon sector, it is common to define the residue of the pole of the f_{ba} amplitude defined in Eq. (50.10) in variable $\sqrt{s}$ instead of s. Accordingly, in the baryon listings the elastic pole residue, which refers to $\pi N \to \pi N$ scattering, is related to the residues introduced above via

$$r_{\pi N,\pi N} = \frac{\rho_{\pi N}(s_{\mathrm{R}})}{\sqrt{4s_{\mathrm{R}}}}\,\mathcal{R}_{\pi N,\pi N}\ , \tag{50.20}$$

where s_{R} is the position of the pole. For evaluation of the phase-space factor for the complex argument, analytic continuation is required.

In the literature there are alternative definitions of a branching fraction, which are more close to what is observed in experiment than what follows from Eq. (50.19). Usually those are defined from the probability of the decay of a resonance to a certain channel as provided by the corresponding amplitude on the real axis, where the measurements are performed. It should be understood that in order to isolate an individual resonance in an amplitude defined on the real axis in general some model dependence is unavoidable (*e.g.* this is possible if the amplitude is provided by a sum of

Breit–Wigner functions, however, since such a sum violates unitarity the parametrisation comes with an intrinsic theoretical uncertainty difficult to quantify). Having that said one may define the partial width of a resonance alternatively via

$$\Gamma_{\mathrm{R}\to a} = \frac{(2\pi)^4}{2M_{\mathrm{R}}} \int |\mathcal{A}_a|^2 \, \mathrm{d}\Phi_a \ , \tag{50.21}$$

where $\mathcal{A}_a$ is the decay amplitude of the resonance into channel a, which for multi-body final states may even contain resonances in a subchannel. For the two-body decay of a narrow, isolated resonance, $\mathcal{A}_a$ is to a good approximation just $\tilde{g}_a$ and we get back to Eq. (50.19). If the mass of the decaying resonance lies below the threshold of the final state, an integration over the resonance lineshape needs to be employed in addition. For example, for some generic three-body decay with two of the final-state particles going through a resonance one commonly defines (avoiding complications from spins or centrifugal barrier factors), for simplicity written in terms of Breit–Wigner functions (see next section)

$$\begin{aligned}\mathrm{Br}_{R\to cR'}\mathrm{Br}_{R'\to ab} = (2\pi)^3 \int_{m^2_{\mathrm{min}R}}^{\infty} dm^2 \left| \frac{g_{R\to R'c}}{M^2_{\mathrm{BW}R} - m^2 - iM_{\mathrm{BW}R}\Gamma_R(m^2)} \right|^2 \\ \times (2\pi)^3 \int_{m^2_{\mathrm{min}R'}}^{(m-m_c)^2} dm^2_{ab} \left| \frac{g_{R'\to ab}}{M^2_{\mathrm{BW}R'} - m^2_{ab} - iM_{\mathrm{BW}R'}\Gamma_{R'}(m^2_{ab})} \right|^2 \int \mathrm{d}\Phi_{ab} \int \mathrm{d}\Phi_{R'(m^2_{ab})c} \ ,\end{aligned} \tag{50.22}$$

where $\Gamma_{R^{(\prime)}}(m^2)$ denotes the energy dependent width of resonance R (R') (details are given in the next section), $\mathrm{d}\Phi_{R'(m^2_{ab})c}$ denotes the two-body phase space for resonance R', at a fixed mass m_{ab}, and particle c for a total energy m, and $\mathrm{d}\Phi_{ab}$ the two-body phase space for particles a and b for a total energy m_{ab}, respectively. Furthermore, $m^2_{\mathrm{min}R^{(\prime)}}$ denotes the threshold of the lightest channel resonance R (R') couples to. For example, employing the parameters of the decay of $N^*(1520)$ to ρN one observes that the equation given above only allows the tail of the ρ-meson to contribute to the partial width of the $N^*(1520)$. If in a certain experiment the kinematics do not allow for a scan of the complete line shape of the mother particle, the appropriate procedure to determine the partial width in the approximation outlined above is to determine the effective resonance parameters from a fit to data and to then evaluate Eq. (50.22) in the limits given there. As stressed above, Eq. (50.22) is correct only, if the use of Breit–Wigner functions is indeed justified for the mother and the daughter particles, which is often not the case. Then, to compare with experiment, the amplitudes need to be parametrised in a more sophisticated way and branching ratios can model independently only be defined via the residues.

In studies of decays where resonance R is very narrow, the first integral in Eq. (50.22) is obsolete and m in the boundaries of the second integral gets fixed to the mass of the mother particle. For recent use of such formulas for B-decays see, e.g., Refs. [45–48]. They were applied to study the three-pion system in Ref. [49].

50.3 Common parameterizations

In general, there is no universal, model-independent recipe to build scattering amplitudes. However, a few approaches presented in this section are practical to extract resonance properties in experimental analyses. The systematic theory uncertainties need to be assessed from a range of model variations that are permitted by general S-matrix principles and that provide a sufficient quality of description of the available data.

50.3.1 *The Breit–Wigner parametrization*

The relativistic Breit–Wigner parametrization provides a propagator for a single, isolated resonance,

$$\mathcal{A}(s) = \frac{N_a(s)}{M_{\rm BW}^2 - s - iM_{\rm BW}\Gamma(s)} \tag{50.23}$$

where $M_{\rm BW}$ is the Breit–Wigner mass, and $\Gamma_{\rm BW} = \Gamma(M_{\rm BW}^2)$ is the Breit–Wigner width. The function $\Gamma(s)$ is determined by the channels that the resonance can decay to. The numerator function $N_a(s)$ is specific to the production process. It includes kinematic factors and couplings related to the production process and the decay. Breit–Wigner functions with a s-independent width are justified only, if there is no relevant threshold in the vicinity of the resonance.

To give a concrete example, we consider a resonance observed in the channel a, that is also coupled to a set of channels labeled by index $b = 1, 2, \ldots$, with the orbital angular momentum l_b. Couplings to the channels are denoted, g_b.

$$N_a(s) = \alpha\, g_a\, n_a(s) \tag{50.24}$$

$$\Gamma(s) = \frac{1}{M_{\rm BW}} \sum_b g_b^2 \rho_b(s) n_b^2(s) \tag{50.25}$$

where the factor $n_a(s)$ includes the kinematic threshold factor q^{l_a}, and the barrier factor $F_{l_a}(q_a/q_0)$ that regularize the high–energy behaviour:

$$n_a = (q_a/q_0)^{l_a} F_{l_a}(q_a/q_0)\,, \tag{50.26}$$

with l_a being the orbital angular momentum in channel a, $q_a(s)$ is defined in Eq. (50.5), and q_0 denotes some conveniently chosen momentum scale. The factor $(q_a)^l$ guarantees the correct threshold behavior. The rapid growth of this factor for angular momenta $l > 0$ is commonly compensated at higher energies by a phenomenological form factor, here denoted by $F_{l_a}(q_a, q_0)$. Often, the Blatt-Weisskopf form factors, $F_j(q/q_0)$, are used [50–52]:

$$\begin{aligned} F_0^2(z) &= 1\,, \\ F_1^2(z) &= 1/(1+z^2)\,, \\ F_2^2(z) &= 1/(9+3z^2+z^4)\,, \end{aligned} \tag{50.27}$$

with the scale parameter $R = 1/q_0$ in the range from $1\,\text{GeV}^{-1}$ to $5\,\text{GeV}^{-1}$. Instead of using coupling constant in Eq. (50.25), one can define the energy-dependent partial width:

$$\Gamma_b(s) = \Gamma_{{\rm BW},b} \frac{\rho_b(s)}{\rho_b(M_{\rm BW}^2)} \left(\frac{q_b}{q_{b\,\rm R}}\right)^{2l_b} \frac{F_{l_b}^2(q_b, q_0)}{F_{l_b}^2(q_{b\,\rm R}, q_0)}\,. \tag{50.28}$$

Here $q_{a\,\rm R}$ are the values of the break-up momentum evaluated at $s = M_{\rm BW}^2$. The substitution is possible only for those channels where the threshold of the decay channel is located below the nominal resonance mass, otherwise, Eq. (50.25) should be used.

The Breit–Wigner parametrization provides an effective description of resonance phenomena. However, the parameters agree with the pole parameters only if the resonance is narrow, isolated (no nearby resonances in the same partial wave) and the background is smooth. Otherwise, the Breit–Wigner parameters deviate from the pole parameters and are reaction-dependent. If there is more than one resonance in one partial wave that significantly couples to the same channel, it is in general incorrect to use a sum of Breit–Wigner functions, for this usually leads to a violation of unitarity constraints, and hence, a non-quantifiable bias to resonance properties which are inferred from the reaction amplitude. In case of overlapping resonances in the same partial wave more refined methods should be used, like the K-matrix approach described in the next section.

50.3.2 *K-matrix approach and Flatté parameterizations*

The K-matrix method is a general construction for coupled-channel scattering amplitudes $\mathcal{M}_{ba}$ that guarantees two-particle unitarity, but does not allow for the inclusion of left-hand cuts [53]. The amplitude reads,

$$n_b \, \mathcal{M}^{-1}_{ba} \, n_a = \mathcal{K}^{-1}_{ba} - i\delta_{ba}\rho_a n_a^2, \tag{50.29}$$

where $\mathcal{K}_{ba}$ is a real function, a subject to modeling. The factor n_a, defined in Eq. (50.26), becomes important for waves with non-zero angular momentum. As there is no unique rigorous recipe to build $\mathcal{K}$, various parameterizations thereof have to be studied, in order to get access to the theoretical systematic uncertainty. One possible choice for the K-matrix is

$$\mathcal{K}_{ba}(s) = \sum_R \frac{g_b^R g_a^R}{m_R^2 - s} + \sum_{i=0}^{N_{\text{b.g.}}} b_{ba}^{(i)} s^i, \tag{50.30}$$

where m_R is referred to as the bare mass of the resonance R (not to be confused with the physical mass), the g_a^R are the bare couplings of the resonance R to the channel a (not to be confused with the residues). The $b_{ba}^{(i)}$ are matrices parameterizing the non-pole parts of the K-matrix. As long as all parameters appearing in Eq. (50.30) are real the amplitude is unitary. From the ansatz given above the scattering amplitude $\mathcal{M}$ can be calculated directly using the matrix form,

$$\mathcal{M} = n[1 - \mathcal{K}\, i\rho\, n^2]^{-1}\mathcal{K}\, n \ , \tag{50.31}$$

where the diagonal matrix in the channel space $n = \text{diag}(n_a, n_b, \dots)$. As an alternative to Eq. (50.30), the same functional form as on the right side of Eq. (50.30) can be used to parameterize the inverse K-matrix, called by authors of Ref. [54] the M-matrix. Many other alternative expressions in the K-matrix framework are used for amplitude studies in lattice-QCD calculations [55–57].

Evaluation of the K-matrix amplitude for the multichannel problem requires an analytic continuation already on the real axis. For a given closed channel c, the factor $q_c(s)$ that enters ρ_c and n_c has to be calculated below the corresponding threshold, *i.e.* in the unphysical region of the particular channel c. This is done using analytic continuation as described *e.g.* in Refs. [27, 58]:

$$q_c = i\sqrt{-q_c^2} \quad \text{for} \quad q_c^2 < 0. \tag{50.32}$$

The resulting line shape above and below the threshold of channel c is called the Flatté parameterization [58]. The contiuation given above stays on the physical sheet. To reach the unphysical sheet the negative square root needs to be chosen. If the coupling of a resonance to the channel opening nearby is very strong, the Flatté parameterization shows a scaling invariance and does not allow for an extraction of individual partial decay widths, but only of ratios [59]. The position of the resonance poles can be determined by a study of the zeros of the analytic function $\det[1 - \mathcal{K}\, i\rho\, n^2]$. Due to the ρ factor, this determinant has a complicated multisheet structure, however, the closest unphysical sheet is always the one which is determined by the heaviest threshold below the studied point in s (*cf.* Fig. 50.2).

50.3.3 *Scattering-length approximation*

A scattering length, a, is defined as the first term in an expansion of the scattering phase shift introduced in Eq. (50.11). For S-waves one finds,

$$q \cot \delta = 1/a + O(q^2) \, , \tag{50.33}$$

where q is the break-up momentum of the scattering system. The sign convention used in Eq. (50.33) is the one commonly employed in particle physics. In this convention a positive scattering length indicates attraction; if, however, the attraction is strong enough to generate a bound

state, the scattering length changes sign and turns negative. A negative scattering length also occurs for repuslive interactions. Note that in nuclear physics the leading term in the expansion of Eq. (50.33) is usually defined as $-1/a$ such that *e.g.* a bound state would be related to a positive scattering length. Employing Eq. (50.33) the scattering amplitude reads

$$\mathcal{M}(s) = \frac{8\pi\sqrt{s}}{1/a - iq(s)} \,. \tag{50.34}$$

The scattering length is proportional to the value of the amplitude at threshold. A scattering length approximation is applicable only in a very limited energy range, however, might well be appropriate to analyse the recently discovered narrow near-threshold states [60,61] from this point of view, *e.g.*, in Refs. [62–64]. Moreover, it is possible to introduce the effect of a weakly coupled lower channel. To see this one might start from

$$\mathcal{K} = \begin{pmatrix} \gamma & \beta \\ \beta & 0 \end{pmatrix} \,, \tag{50.35}$$

with β, γ being real numbers. It leads to

$$\mathcal{M}_{\text{el.}}(s) = \frac{1}{1/(\gamma + i\beta^2\rho_{\text{inel.}}(s)) - i\rho(s)} \,, \tag{50.36}$$

with $\rho_{\text{inel.}}(s)$ being the phase-space factor of the inelastic channel. The scattering length for the amplitude in Eq. (50.36) obtains an imaginary part due to the coupling to the lower channel,

$$a = \frac{1}{8\pi\sqrt{s_{\text{thr}}}} \left(\gamma + i\beta^2\rho_{\text{inel.}}(s_{\text{thr}})\right) \,. \tag{50.37}$$

If the function $\beta^2\rho_{\text{inel.}}(s)$ does not vary significantly in the energy range studied, the scattering-length approximation with a complex value is justified. For large values of a the amplitude of Eq. (50.36) develops a near-threshold pole located on the physical or unphysical sheet for negative or positive values of γ, respectively. While easy to use, it is important to stress, however, that the approximation in Eq. (50.35) is a specific choice of the dynamic function that produces a single pole near the physical region pointing at a hadronic molecule nature of the state studied [64–67]. Virtual states are discussed in this context in Ref. [68]. For practical analyses, various modifications of the parameterization have to be tested.

50.3.4 *Two methods to build the production amplitude*

When the unitary scattering amplitude is fixed, it can be used to build the production amplitude in a way that it is consistent with unitarity [52,69].

1. The **Q-vector** approach is discussed in Ref. [52,54,70]. It reads,

$$\mathcal{A}_a(s) = \sum_c \mathcal{M}_{ac}(s) Q_c(s)/n_c, \qquad Q_c(s) = \sum Q_c^{(i)} s^i. \tag{50.38}$$

The unitarity condition of Eq. (50.14) is satisfied when $Q_c(s)$ is a real function and in particular does not have singularities above the lowest threshold for all channels c. Besides these conditions $Q_c(s)$ is arbitrary. Note that in the Q-vector approach the left hand cuts of the scattering matrix $\mathcal{M}_{ac}(s)$ get imported to the production amplitude which might generate a wrong analytic structure. If this problem is relevant needs to be investigated on a case-by-case basis. In a study of $\gamma\gamma \to \pi\pi$, *cf.* Ref. [41,42] a low-order polynomial is claimed to be sufficient to parametrize the energy dependence of the function $Q_c(s)$. The Q-vector method is convenient, if the full matrix $\mathcal{M}$ is known, *cf.* Ref. [54].

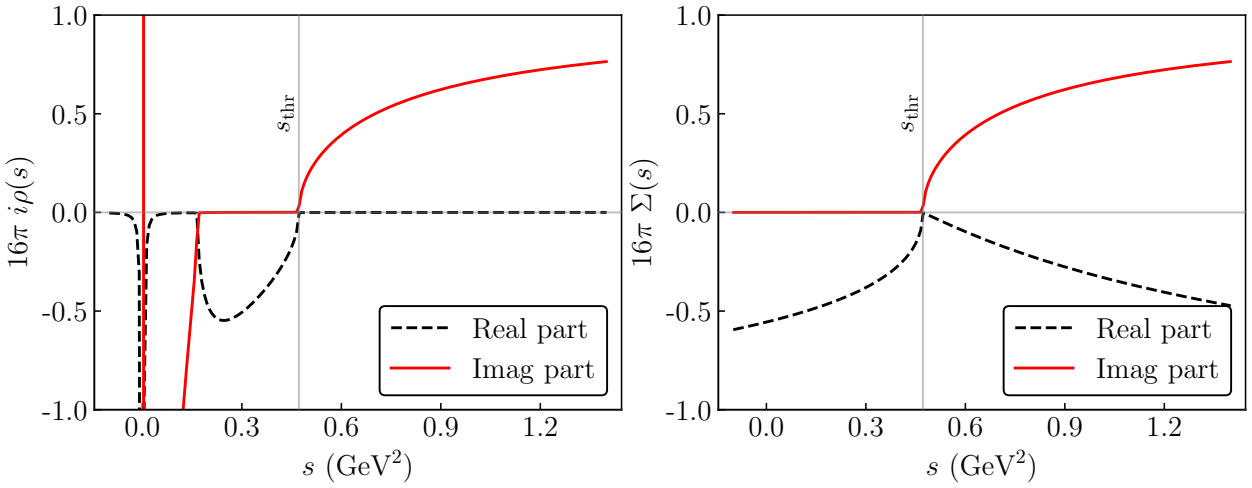

Figure 50.4: Comparison of the $i\rho$ function (left plot) to the Chew-Mandelstam function from Eq. (50.40) (right plot), evaluated for the case of S-wave $\eta\pi$ scattering. The values of s are taken slightly above the real axis, $s + i0$. The solid red line shows the imaginary part that is the same for both functions above threshold. The dashed black line presents the real part. One finds indications of the unphysical left-hand singularities of the function $i\rho$ on the left plot, while the Chew-Mandelstam function in analytic below the two-particle threshold.

2. The ***P*-vector** is a parameterization that exploits the K-matrix of the scattering amplitude [53, 69]. It contains two components: the background term B_c that is coupled to the K-matrix via an intermediate loop represented by the $i\rho$ factor, and the "direct" resonance production term with couplings α_c^R:

$$\mathcal{A}_a(s) = n_a \sum_c \left[1 - \mathcal{K}\, i\rho n^2\right]^{-1}_{ac} P_c, \qquad P_c = \sum_R \frac{\alpha^R g_c^R}{m_R^2 - s} + B_c. \tag{50.39}$$

   Again, unitarity requires the parameters B_c and α^R to be real.Here, the masses m_R and the couplings g_c^R need to agree with those in $\mathcal{K}$ in Eq. (50.30).

An important difference between the methods is to be noticed [69]. When the two-particle scattering amplitude goes to zero, the production amplitude in the Q–vector method vanishes for finite values of Q_c, while it stays finite in the P-vector approach. An version of the P-vector approach that exploits the analytic properties of production amplitudes [69, 71, 72] is widely used, *e.g.* in the dispersive Khuri-Treiman framework [28, 73] for the construction of three-body-decay amplitudes.

50.3.5 *Further improvements: Chew-Mandelstam function*

The K-matrix described above usually allows one to get a proper fit of physical amplitudes and it is easy to deal with, however, it also has an important deficit: it violates constraints from analyticity — *e.g.*, ρ_a, given by Eq. (50.9), is ill-defined at $s = 0$, and for unequal masses it develops an unphysical cut (see left panel of Fig. 50.4). A method to improve the analytic properties was suggested in Refs. [74–78]. It replaces the phase-space factor $i\rho_a(s)$ in Eq. (50.29) by the analytic function $\Sigma_a(s)$ that produces the identical imaginary part on the right-hand cut. This function is called the Chew-Mandelstam function and for S-waves it reads [72, 76]:

$$\Sigma_a(s) = \frac{1}{16\pi^2}\left[\frac{2q_a}{\sqrt{s}} \log \frac{m_1^2 + m_2^2 - s + 2\sqrt{s}q_a}{2m_1 m_2} - (m_1^2 - m_2^2)\left(\frac{1}{s} - \frac{1}{(m_1+m_2)^2}\right)\log\frac{m_1}{m_2}\right], \tag{50.40}$$

where m_1 and m_2 are masses of the final-state particles in channel a, $s_{\text{thr}_a} = (m_1 + m_2)^2$. The function along the real axis is plotted in the right panel of Fig. 50.4. For channels with $j > 0$, the threshold behavior has to be incorporated properly. This can be done, *e.g.*, by computing the dispersion integral

$$\Sigma_a(s + i0) = \frac{s - s_{\text{thr}_a}}{\pi} \int_{s_{\text{thr}_a}}^{\infty} \frac{\rho_a(s') n_a^2(s')}{(s' - s_{\text{thr}_a})(s' - s - i0)} \, \mathrm{d}s' . \tag{50.41}$$

A further discussion of the calculation of the Chew-Mandelstam function can be found in Refs. [79, 80].

If there is only a single resonance in a given channel, it is possible to feed the imaginary part of the Breit–Wigner function, Eq. (50.23) with an energy-dependent width, directly into a dispersion integral to get a resonance propagator with the correct analytic structure [81, 82].

50.3.6 *Two-potential decomposition*

Another advanced technique to construct the scattering amplitude which is widely used in the literature [83–87] is based on the two-potential formalism [88]. The method is usually formulated for the full unprojected amplitude $\mathcal{M}_{ba}(s, t)$, however, in order to simplify the discussion we present the equations in the partial-wave-projected form.

The scattering amplitude $\mathcal{M}$ is decomposed into a pole part and a non-pole part, often called background (b.g.)

$$\mathcal{M}(s) = \mathcal{M}^{\text{b.g.}}(s) + \mathcal{M}^{\text{pole}}(s) . \tag{50.42}$$

The splitting given in Eq. (50.42) is not unique and model-dependent (see, *e.g.*, the discussions in Refs. [89, 90]). The background scattering matrix is assumed to be unitary by itself. One option is to parameterize it, *e.g.* at low energies directly in terms of phase shifts and inelasticities — see, *e.g.*, Refs. [44, 87, 91]. In this case the vertex functions $\Omega(s)_{ab}$ introduced below can be written in terms of an Omnes matrix [91], which reduces to the well-known Omnes function in the single-channel case [71]. Alternatively, it can be computed based on some potential, $V^{\text{b.g.}}$, fed into a proper scattering equation.

The complete amplitude $\mathcal{M}$ of Eq. (50.42) is unitary, if the pole part is chosen as

$$\mathcal{M}^{\text{pole}}(s) = \Omega(s) \, [1 - V^{\text{R}}(s) \Sigma^u(s)]^{-1} V^{\text{R}}(s) \, \Omega^T(s) \, . \tag{50.43}$$

where the resonance potential reads in channel space

$$V^{\text{R}}_{ab}(s) = \sum_R \frac{g_a^R \, g_b^R}{M_R^2 - s} \, , \tag{50.44}$$

Σ^u_{ab} denotes the self-energy matrix, and g_a^R and M_R denote the bare coupling of the resonance R to channel a and its bare mass, respectively. A relation analogous to Eq. (50.6) holds for the normalized vertex functions, however, with the final state interaction provided by $\mathcal{M}^{\text{b.g.}}$

$$\text{Disc} \, \Omega_{ab}(s) = 2i \sum_c \mathcal{M}^{\text{b.g.}\,*}_{ca}(s) \, \rho_c(s) \, \Omega_{cb}(s) \, . \tag{50.45}$$

The discontinuity of the self-energy matrix $\Sigma^u(s)$ is

$$\text{Disc} \, \Sigma^u_{ab}(s) = 2i \sum_c \Omega^*_{ca}(s) \, \rho_c(s) \, \Omega_{cb}(s) \, . \tag{50.46}$$

The real part of Σ^u can be calculated from Eq. (50.46) via a properly subtracted dispersion integral. If $\mathcal{M}^{\text{b.g.}}$ is unitary, the use of Eq. (50.43) leads to a unitary full amplitude, *cf.* Eq. (50.42). However,

the pole term alone is unitary only for a vanishing background amplitude. In this situation the amplitude just described reduces to the analytically improved K-matrix of Sec. 50.3.5. While the omission of non-pole terms is a bad approximation for, *e.g.*, scalar-isoscalar $\pi\pi$ interactions at low energies [92], it typically works well for higher partial waves.

The algebra of the two potential splitting presented in Eq. (50.42) is found to be very practical in various other cases, beyond the pole-background separation. It was employed in Refs. [87, 91] to treat the pion vector and scalar form factor, respectively, over a sizable energy range including inelasticities. A similar decomposition applied to the $3 \to 3$ scattering problem provided a way to isolate the non-separable one-particle exchange singularity from the short-range resonance interaction [93].

Acknowledgement

We are very grateful to Mikhail Mikhasenko, who gave vital input to improve this review and to Ulf-G. Meißner for valuable comments on the manuscript.

References

[1] M. Jacob and G. C. Wick, Annals Phys. **7**, 404 (1959), [Annals Phys.281,774(2000)].

[2] C. Zemach, Phys. Rev. **140B**, 97, 109 (1965).

[3] A. V. Anisovich *et al.*, J. Phys. **G28**, 15 (2002), [hep-ph/0105330].

[4] V. N. Gribov, Y. L. Dokshitzer and J. Nyiri, *Strong Interactions of Hadrons at High Energies – Gribov Lectures on Theoretical Physics*, Cambridge University Press, Cambridge (2009).

[5] L. Landau, Nucl. Phys. **13**, 181 (1959).

[6] R. Cutkosky, J. Math. Phys. **1**, 429 (1960).

[7] A rapid change in an amplitude is not an unambiguous signal of a singularity of the S–matrix [94], however, for realistic interactions this connection holds.

[8] S. Coleman and R. E. Norton, Nuovo Cim. **38**, 438 (1965).

[9] C. Schmid, Phys. Rev. **154**, 5, 1363 (1967).

[10] I. J. R. Aitchison and C. Kacser, Il Nuovo Cimento A (1965-1970) **40**, 2, 576 (1965), ISSN 1826-9869, URL https://doi.org/10.1007/BF02721045.

[11] M. Mikhasenko, B. Ketzer and A. Sarantsev, Phys. Rev. **D91**, 9, 094015 (2015), [arXiv:1501.07023].

[12] M. Bayar *et al.*, Phys. Rev. **D94**, 7, 074039 (2016), [arXiv:1609.04133].

[13] F. Aceti, L. R. Dai and E. Oset, Phys. Rev. **D94**, 9, 096015 (2016), [arXiv:1606.06893].

[14] J.-J. Wu *et al.*, Phys. Rev. Lett. **108**, 081803 (2012), [arXiv:1108.3772].

[15] L. D. Roper, Phys. Rev. Lett. **12**, 340 (1964).

[16] M. Fukugita and K. Igi, Phys. Rept. **31**, 237 (1977).

[17] S. M. Roy, Phys. Lett. **36B**, 353 (1971).

[18] B. Ananthanarayan *et al.*, Phys. Rept. **353**, 207 (2001), [hep-ph/0005297].

[19] G. Colangelo, J. Gasser and H. Leutwyler, Nucl. Phys. **B603**, 125 (2001), [hep-ph/0103088].

[20] R. Garcia-Martin *et al.*, Phys. Rev. **D83**, 074004 (2011), [arXiv:1102.2183].

[21] P. Buettiker, S. Descotes-Genon and B. Moussallam, Eur. Phys. J. **C33**, 409 (2004), [hep-ph/0310283].

[22] M. Hoferichter, D. R. Phillips and C. Schat, Eur. Phys. J. **C71**, 1743 (2011), [arXiv:1106.4147].

[23] G. E. Hite and F. Steiner, Nuovo Cim. A **18**, 237 (1973).

[24] M. Hoferichter *et al.*, Phys. Rept. **625**, 1 (2016), [arXiv:1510.06039].

[25] M. P. Peskin and D. V. Schroeder, *An Introduction to Quantum Field Theory*, Westview Press, 1995.

[26] R. Garcia-Martin *et al.*, Phys. Rev. D **83**, 074004 (2011), [arXiv:1102.2183].

[27] V. V. Anisovich and A. V. Sarantsev, Eur. Phys. J. **A16**, 229 (2003), [hep-ph/0204328].

[28] N. N. Khuri and S. B. Treiman, Phys. Rev. **119**, 1115 (1960).

[29] J. Kambor, C. Wiesendanger and D. Wyler, Nucl. Phys. B **465**, 215 (1996), [hep-ph/9509374].

[30] A. V. Anisovich and H. Leutwyler, Phys. Lett. B **375**, 335 (1996), [hep-ph/9601237].

[31] P. Guo *et al.*, Phys. Lett. **B771**, 497 (2017), [arXiv:1608.01447].

[32] M. Albaladejo and B. Moussallam, Eur. Phys. J. **C77**, 8, 508 (2017), [arXiv:1702.04931].

[33] G. Colangelo *et al.*, Eur. Phys. J. **C78**, 11, 947 (2018), [arXiv:1807.11937].

[34] K. Kampf *et al.*, Phys. Rev. D **101**, 7, 074043 (2020), [arXiv:1911.11762].

[35] F. Niecknig, B. Kubis and S. P. Schneider, Eur. Phys. J. **C72**, 2014 (2012), [arXiv:1203.2501].

[36] I. V. Danilkin *et al.*, Phys. Rev. **D91**, 9, 094029 (2015), [arXiv:1409.7708].

[37] T. Isken *et al.*, Eur. Phys. J. **C77**, 7, 489 (2017), [arXiv:1705.04339].

[38] F. Niecknig and B. Kubis, JHEP **10**, 142 (2015), [arXiv:1509.03188].

[39] F. Niecknig and B. Kubis, Phys. Lett. **B780**, 471 (2018), [arXiv:1708.00446].

[40] K. M. Watson, Phys. Rev. **95**, 228 (1954).

[41] D. Morgan and M. R. Pennington, Z. Phys. **C37**, 431 (1988), [Erratum: Z. Phys.C39,590(1988)].

[42] D. Morgan and M. R. Pennington, Z. Phys. **C48**, 623 (1990).

[43] B. Moussallam, Eur. Phys. J. C **71**, 1814 (2011), [arXiv:1110.6074].

[44] L. Von Detten *et al.*, Eur. Phys. J. C **81**, 5, 420 (2021), [arXiv:2103.01966].

[45] R. Aaij *et al.* (LHCb), Phys. Rev. D **94**, 7, 072001 (2016), [arXiv:1608.01289].

[46] R. Aaij *et al.* (LHCb), Phys. Rev. D **92**, 1, 012012 (2015), [arXiv:1505.01505].

[47] R. Aaij *et al.* (LHCb), Phys. Rev. D **91**, 9, 092002 (2015), [Erratum: Phys.Rev.D 93, 119901 (2016)], [arXiv:1503.02995].

[48] R. Aaij *et al.* (LHCb), Phys. Rev. D **102**, 112003 (2020), [arXiv:2009.00026].

[49] M. Aghasyan *et al.* (COMPASS), Phys. Rev. D **98**, 9, 092003 (2018), [arXiv:1802.05913].

[50] J. M. Blatt and V. F. Weisskopf, *Theoretical nuclear physics*, Springer, New York (1952), ISBN 9780471080190.

[51] F. Von Hippel and C. Quigg, Phys. Rev. **D5**, 624 (1972).

[52] S. U. Chung *et al.*, Annalen Phys. **4**, 404 (1995).

[53] I. J. R. Aitchison, Nucl. Phys. **A189**, 417 (1972).

[54] K. L. Au, D. Morgan and M. R. Pennington, Phys. Rev. **D35**, 1633 (1987).

[55] J. J. Dudek, R. G. Edwards and D. J. Wilson (Hadron Spectrum), Phys. Rev. **D93**, 9, 094506 (2016), [arXiv:1602.05122].

[56] R. A. Briceno *et al.*, Phys. Rev. **D97**, 5, 054513 (2018), [arXiv:1708.06667].

[57] A. J. Woss *et al.* (2019), [arXiv:1904.04136].

[58] S. M. Flatte, Phys. Lett. **63B**, 224 (1976).

[59] V. Baru *et al.*, Eur. Phys. J. **A23**, 523 (2005), [arXiv:nucl-th/0410099].

[60] S. K. Choi *et al.* (Belle), Phys. Rev. Lett. **91**, 262001 (2003), [hep-ex/0309032].

[61] R. Aaij *et al.* (LHCb), Phys. Rev. Lett. **122**, 22, 222001 (2019), [arXiv:1904.03947].

[62] E. Braaten and J. Stapleton, Phys. Rev. **D81**, 014019 (2010), [arXiv:0907.3167].

[63] V. Baru *et al.*, Eur. Phys. J. **A44**, 93 (2010), [arXiv:1001.0369].

[64] C. Fernández-Ramírez *et al.* (JPAC), Phys. Rev. Lett. **123**, 9, 092001 (2019), [arXiv:1904.10021].

[65] D. Morgan, Nucl. Phys. **A543**, 632 (1992).

[66] V. Baru *et al.*, Phys. Lett. **B586**, 53 (2004), [hep-ph/0308129].

[67] F.-K. Guo *et al.*, Rev. Mod. Phys. **90**, 1, 015004 (2018), [arXiv:1705.00141].

[68] I. Matuschek *et al.*, Eur. Phys. J. A **57**, 3, 101 (2021), [arXiv:2007.05329].

[69] I. J. R. Aitchison (2015), [arXiv:1507.02697].

[70] R. N. Cahn and P. V. Landshoff, Nucl. Phys. **B266**, 451 (1986).

[71] R. Omnes, Nuovo Cim. **8**, 316 (1958).

[72] J. L. Basdevant and E. L. Berger, Phys. Rev. **D16**, 657 (1977).

[73] I. J. R. Aitchison and R. Pasquier, Phys. Rev. **152**, 4, 1274 (1966).

[74] G. J. Gounaris and J. J. Sakurai, Phys. Rev. Lett. **21**, 244 (1968).

[75] M. R. Pennington *et al.*, Eur. Phys. J. **C56**, 1 (2008), [arXiv:0803.3389].

[76] J. A. Oller and E. Oset, Phys. Rev. **D60**, 074023 (1999), [hep-ph/9809337].

[77] N. N. Achasov and A. V. Kiselev, Phys. Rev. **D83**, 054008 (2011), [arXiv:1011.4446].

[78] A. V. Anisovich *et al.*, Phys. Rev. **D84**, 076001 (2011).

[79] J. H. Reid and N. N. Trofimenkoff, J. Math. Phys. **25**, 3540 (1984).

[80] J. A. Oller and U. G. Meissner, Phys. Lett. B **500**, 263 (2001), [hep-ph/0011146].

[81] E. L. Lomon and S. Pacetti, Phys. Rev. **D85**, 113004 (2012), [Erratum: Phys. Rev.D86,039901(2012)], [arXiv:1201.6126].

[82] B. Moussallam, Eur. Phys. J. **C73**, 2539 (2013), [arXiv:1305.3143].

[83] I. R. Afnan and B. Blankleider, Phys. Rev. **C22**, 1638 (1980).

[84] A. D. Lahiff and I. R. Afnan, Phys. Rev. **C60**, 024608 (1999), [arXiv:nucl-th/9903058].

[85] A. Matsuyama, T. Sato and T. S. H. Lee, Phys. Rept. **439**, 193 (2007), [arXiv:nucl-th/0608051].

[86] D. Ronchen *et al.*, Eur. Phys. J. **A49**, 44 (2013), [arXiv:1211.6998].

[87] C. Hanhart, Phys. Lett. **B715**, 170 (2012), [arXiv:1203.6839].

[88] K. Nakano, Phys. Rev. **C26**, 1123 (1982).

[89] D. Djukanovic, J. Gegelia and S. Scherer, Phys. Rev. **D76**, 037501 (2007), [arXiv:0707.2030].

[90] M. Doring *et al.*, Phys. Lett. **B681**, 26 (2009), [arXiv:0903.1781].

[91] S. Ropertz, C. Hanhart and B. Kubis, Eur. Phys. J. **C78**, 12, 1000 (2018), [arXiv:1809.06867].

[92] J. Gasser and U. G. Meissner, Nucl. Phys. **B357**, 90 (1991).

[93] M. Mikhasenko *et al.*, JHEP **08**, 080 (2019), [arXiv:1904.11894].

[94] G. Calucci, L. Fonda and G. C. Ghirardi, Phys. Rev. **166**, 1719 (1968).